Journal of Cardiovascular Computed Tomography xxx (xxxx) xxx

Contents lists available at ScienceDirect

Journal of Cardiovascular Computed Tomography

journal homepage: www.JournalofCardiovascularCT.com

Research paper

Specific calcium deposition on pre-procedural CCTA at the time of percutaneous coronary intervention predicts in-stent restenosis in symptomatic patients☆

Rafael Adolf [a], Insa Krinke [a], Janina Datz [b,d], Salvatore Cassese [b], Adnan Kastrati [b], Michael Joner [b], Heribert Schunkert [b,c], Wolfgang Wall [d], Martin Hadamitzky [a], Leif-Christopher Engel [b,*]

[a] Institut für Radiologie und Nuklearmedizin, Deutsches Herzzentrum München, Klinik an der Technischen Universität München, Lazarettstrasse 36, 80636 Munich, Germany
[b] Klinik für Herz- und Kreislauferkrankungen, Deutsches Herzzentrum München, Klinik an der Technischen Universität München, Lazarettstrasse 36, 80636 Munich, Germany
[c] German Center for Cardiovascular Research (DZHK), Partner Site Munich Heart Alliance, Munich, Germany
[d] Institute for Computational Mechanics, Technical University of Munich, 85748 Garching b., München, Germany

ARTICLE INFO

Keywords:
In-stent restenosis
Coronary computed tomography angiography
Pericoronary adipose tissue

ABSTRACT

Purpose: To characterize preprocedural coronary atherosclerotic lesions derived from CCTA and assess their association with in-stent restenosis (ISR) after percutaneous coronary intervention (PCI).
Materials and methods: This retrospective cohort-study included patients who underwent CCTA for suspected coronary artery disease, subsequent index angiography including PCI and surveillance angiography within 6–8 months after the index procedure. We performed a plaque analysis of culprit lesions on CCTA using a dedicated plaque analysis software including assessment of the surrounding pericoronary fat attenuation index (FAI) and compared findings between lesions with and without ISR at surveillance angiography after stenting.
Results: Overall 278 coronary lesions in 209 patients were included. Of these lesions, 43 (15.5 %) had ISR at surveillance angiography after stenting while 235 (84.5 %) did not. Likewise, plaque composition such as volume of calcification [129.8 mm^3 (83.3–212.6) vs. 94.4 mm^3 (60.4–160.5) p = 0.06] and lipid-rich and fibrous plaque volume [38.4 mm^3 (19.4–71.2) vs. 38.0 mm^3 (14.0–59.1), p = 0.11 and 50.4 mm^3 (26.1–77.6) vs. 42.1 mm^3 (31.1–60.3), p = 0.16] between lesion with and without ISR were not statistically significant. However lesions associated with ISR were more eccentric (n = 37, 86.0 % versus n = 159, 67,7 %; p = 0.03) and more frequently demonstrated calcified portions on opposite sides on the vessel wall on cross-sectional datasets (n = 24, 55.8 % versus n = 55, 23.4 %, p = 0.001). FAI_{lesion} was significantly different in lesions with ISR as compared to those without ISR [-76.5 (−80.1 to −73.6) vs. −80.9 (−88.9 to −74.0), p = 0.02]. There was no difference with respect to FAI_{RCA} between the two groups [-77.4 (−81.9 to −75.6) vs. −78.5 (−86.0 to −71.0), p = 0.41].
Conclusion: Coronary lesions associated with ISR at surveillance angiography demonstrated differences in the arrangement of calcified portions as well as an increased lesion-specific pericoronary fat attenuation index at baseline CCTA. This latter finding suggests that perivascular inflammation at baseline may play a major role in the development of in-stent restenosis.

1. Introduction

Percutaneous coronary intervention (PCI) with stent placement is a standard therapy for myocardial revascularization of hemodynamically significant coronary artery disease (CAD).[1] Despite major improvements in stent technology in the last decades, stent-related events such as thrombosis, myocardial infarction (MI) and in-stent restenosis requiring repeat revascularization continue to occur at a rate of around 2 % per year up to 5 years after PCI with all metallic stents.[2] Drug-eluting stents

☆ The data underlying this article cannot be shared publicly due to the privacy of individuals that participated in the study. The data will be shared on reasonable request to the corresponding author.

* Corresponding author.
E-mail address: leifengel@hotmail.com (L.-C. Engel).

https://doi.org/10.1016/j.jcct.2024.09.010
Received 18 February 2024; Received in revised form 28 July 2024; Accepted 26 September 2024

Abbreviations

BMI	Body mass index
CAD	Coronary artery disease
CAC	Coronary artery calcium
CCTA	Coronary CT angiography
CI	Confidence interval
CPV	Calcified plaque volume
FAI	Fat attenuation index
ICA	Invasive catheter angiography
ISR	In-stent restenosis
IVUS	Intravascular ultrasound
LAD	Left anterior descending
LCX	Left circumflex artery
LL	Lesion length
LM	Left main
MI	Myocardial infarction
NCPV	Non-calcified plaque volume
NPV	Negative predictive value
OR	Odds ratio
PCAT	Pericoronary adipose tissue
PVAT	Perivascular adipose tissue
PPV	Positive predictive value
QCA	Quantitative coronary angiography
RCA	Right coronary artery
RI	Remodeling index
SD	Standard deviation
TPV	Total plaque volume

(DES) with antiproliferative drugs reduced the incidence of in-stent restenosis (ISR) when compared with bare metal stents (BMS), nevertheless 5 %–10 % of patients with DES are diagnosed with ISR[3–5]

So far many risk factors for the development of ISR have been identified, which can currently be categorized into patient-related, stent-related and procedure-related causes.[5,6] Beyond that, it has been postulated that lesion-related factors prior to the stenting-procedure such as plaque-composition may contribute to the development of ISR.[7–9] Additionally, vascular inflammation plays a major role not only in atherosclerotic plaque formation, but also in the development and progression of in-stent restenosis.[10–13]

Changes in pericoronary adipose tissue composition can be detected through CT images as vascular inflammation shifts perivascular adipose tissue (PVAT) attenuation from more fatty (around −190 HU) to less fatty (around −30 HU) values due suppression of adipose cell differentiation.[14–18] Fat attenuation index (FAI) of the pericoronary adipose tissue on coronary computed tomography angiography (CCTA) is a validated surrogate marker of inflammation on CT-images with prognostic implications in regards to major adverse cardiac events.[19] The goal of this study was to characterize preprocedural coronary atherosclerotic lesions derived from coronary computed tomography angiography (CCTA) and assess their association with in-stent restenosis after percutaneous coronary intervention (PCI).

2. Materials and Methods

2.1. Study population

In this study, coronary CT angiography and invasive catheterization databases at the German Heart Center in Munich, Germany were screened for patients with suspected or known CAD who had undergone coronary CTA due to suspected coronary artery disease between 2011 and 2016 and received subsequent invasive angiography including percutaneous coronary intervention (PCI) with stent implantation as well as surveillance angiography within 6–8 months after index procedure.

Patients with acute coronary syndrome or hemodynamic instability, a lack of stable sinus rhythm during the examination, prior stent implantation or coronary bypass surgery were excluded from analyses. Before examination, a structured patient characterization was performed, including patient age, height and weight, as well as history of cardiac disease, present concerns and current medication. The study design was approved by the local ethics committee.

2.2. Image acquisition

CCTA images were acquired on a 128-slice dual source CT system from January 2011 to May 2014 and a 192-slice dual source CT system from June 2014 to December 2018 (Siemens Heathineers, Erlangen, Germany).

According to the patient's heart rate and absence of contraindications intravenous beta-blocker medication was administered targeting a heart rate less than 60 beats/min. Sublingual nitrates were applied if systolic blood pressure was higher than 100 mmHg.

The coronary prospective ECG-synchronized CTA was triggered into the diastolic phase (70 % of RR-interval) and performed in a single-acquisition, high-pitch protocol. Tube voltage was selected by the technician and/or physician between 70 and 120 kVp, tube current was adapted automatically based on body size (CARE Dose). Contrast circulation time was determined using a testbolus with 10 ml contrast media (Imeron 350, Bracco Imaging GmbH, Konstanz, Germany), followed by a 50 ml 0.9 % saline chaser. The coronary CT angiogram was performed with a 50 ml contrast bolus at 5.0 ml/s, followed by 30 ml 0.9 % saline chaser.

Axial image reconstructions were performed in the cardiac end-diastolic phase using a slice thickness of 0.6 mm, increment of 0.4 mm.

2.3. Assessment of CCTA data and quantitative markers

A dedicated semi-automatic software prototype was used for the analysis of morphological characteristics (Coronary Plaque Analysis 2.0.3, Syngo.via VA30, Siemens Erlangen, Germany).

After automated segmentation with automatic vessel centerline extraction and anatomical labeling of the main vessels, semi-automated inner- and outer-wall delineation were performed in curved multiplanar reformations (CPR), using the cross-sectional views for manual optimization to avoid small side branches or coronary veins.

Culprit lesions resulting in an index PCI with stent placement were independently analyzed on the initial coronary CT angiography by two observers (R.A. and L.-C.E.) who were blinded to the patients' history. Discordant cases were resolved by a consensus reading.

As the reference for diameter and area stenosis determination, average dimensions of non-affected vessel segments immediately proximal and distal to the lesion of interest were measured at sections free of atherosclerotic plaque.

This analysis software uses automated segmentation based on attenuation values prevailing in the target anatomy within user-defined proximal and distal boundaries to compute a comprehensive array of quantitative atherosclerosis lesion description.

In accordance with current guidelines,[20,21] the location of the target lesion was determined using the first 15 of the original 18 segments according to the simplified American Heart Association classification.[22] Coronary artery luminal stenosis was graded as none (0 %), minimal (1%–24 %), mild (25%–49 %), moderate (50%–69 %), severe (≥70 %) and totally occluded.

Total plaque volume, calcified, lipid-rich and fibrous plaque volumes were automatically measured by the software with the following cut-off values (HU) for the different plaque characteristics: Non-calcified plaque

components were considered lipid-rich when its attenuation ranges between −100 and 70 HU and considered as fibrotic when showing an attenuation between 71 and 124 HU. Plaque components were defined as calcified when showing an attenuation above 125 HU.[23]

Culprit vessels were described as diffuse diseased if the coronary vessel wall had continuous atherosclerotic plaque burden without intermittent parts of healthy vessel wall. All coronary atherosclerotic lesions were categorized into non-calcified, calcified and partially calcified plaques and described as asymmetric if the plaque portion did not involve the entire circumference of the coronary artery. Similarly, for calcified plaques or calcified plaque areas, we used the term eccentric if the if more than 50 % of the calcification did not involve the entire circumference of the coronary artery as assessed qualitatively. Calcified plaques were further characterized as "spotty" if the diameter was less than 3 mm in any direction, and as homogenous if the attenuation within the calcification was uniform. Additionally, after thorough co-registration between noninvasive and invasive procedures and mirroring the exact site of maximum catheterization in-stent restenosis on CCTA, we analyzed the exact position of calcification at this very location: In case calcified portions were located on opposite sides on the vessel wall on cross-sectional CCTA images, we labeled this CT signature headlight *sign* (i.e. we chose this name due to its resemblance of the bright front headlights of a car). On vessel cross-sections, remodeling index (RI) was calculated as the ratio of the maximal vessel diameter and its closest proximal (or distal, in ostial lesions) normal reference vessel lumen diameter.[24]

2.4. Pericoronary adipose tissue (PCAT) analysis on CT datasets

Lesion and vessel-specific pericoronary adipose tissue attenuation was measured radially outward from the outer coronary wall in predefined regions, only considering voxels between −190 and −30 HU within a distance from the outer vessel wall that is similar to the inner vessel diameter, as shown previously.[19]

FAI was defined as the mean attenuation of the included adipose tissue voxels. FAI_{RCA} analysis focused on the proximal segment (10–50 mm) from the ostium of the RCA. Similarly, FAI_{lesion} was quantified within a 40 mm - segment covering the culprit-lesion. Side branches adjacent to the vessel wall were excluded from FAI analysis.

2.5. Invasive procedures

Following CCTA, each patient underwent subsequent invasive workup including an index angiography with percutaneous coronary intervention (PCI) as well as subsequent surveillance angiography within 6–8 months after the index procedure using standard techniques. During both index and surveillance angiography, at least two views of each major epicardial vessel using the same projections were obtained. In-stent restenosis was defined as lesions with at least 50 % luminal narrowing and treated with recurrent PCI based on the decision of the interventional cardiologist.

2.6. Statistical analysis

For statistical analysis, SPSS - software version 24 (SPSS Statistics, IBM, Armonk, New York) was used. Results are expressed as mean standard deviation (SD) or median (range) for non-normally distributed data. An unpaired Student *t*-test and Mann-Whitney *U* test was applied for comparison of continuous and non-normally distributed variables, respectively. Categorical variables were compared by the chi-square-test. Univariate and multivariate logistic regression analysis was performed to assess the relationship of baseline CCTA characteristics on the primary outcome of in-stent restenosis. We used backward elimination as the basis for multivariate regression, where the variable with the highest p-value is removed from the model. This process is repeated until all variables in the model have a p-value below <0.05, which was considered statistically significant. Categorical variables between the groups were compared using the chi-square test. Groups were compared using the chi-square test.

3. Results

3.1. Patient characteristics

A total of 209 patients were included, with a mean age of 65.1 ± 10.3 years, and n = 171 (81.8 %) were male. Overall n = 34 (16.3 %) patients had an ISR at surveillance angiography after stenting. At least one coronary lesion on CCTA that triggered further invasive testing, was present in n = 155 (74.2 %) patients. At least two lesions were present in n = 41 (19.6 %). Three and more lesions in the coronary tree were seen in n = 9 (4.3 %) and n = 4 (1.9 %), respectively. Baseline clinical characteristics including cardiovascular risk factors, laboratory results and medications were similar between patients with and w/o in-stent restenosis and are shown in Table 1. Out of n = 34 patients with ISR, optical coherence tomography (OCT) was performed.

Preprocedural qualitative and quantitative CCTA lesion characteristics can be seen in the Supplemental Table 1.

3.2. CT-derived lesion characteristics

Overall 278 lesions were included for CCTA analysis. The majority of lesions were located in the left anterior descending artery (LAD; n = 155, 55.8 %), followed by the right coronary artery (RCA; n = 76, 27.3 %), the left circumflex artery (LCX; n = 41, 14.7 %) and the left main stem (LM; n = 6, 2.2 %). Of these, 43 (15.5 %) had ISR at surveillance angiography while 235 (84.5 %) did not. Both ISR and non-ISR lesions did not differ with respect to its length (27.9 ± 9.8 mm versus 27.6 ± 6.73 mm; p = 0.40) the degree of stenosis (74.0 ± 18.5 % versus 71.4 ± 20.4 %; p = 0.15), minimal lumen area [MLA; 1.70 (0.87–3.05) versus 1.91 (1.19–2.53), p = 0.33] or the remodeling index (0.99 versus 1.05, p = 0.22). Additionally both types of lesions were equally likely to be part of diffusely diseased vessels (51.2 % vs. 38.3 %; p = 0.009). Plaque composition between lesions with and w/o ISR at surveillance angiography was similar, meaning that differences in calcified [129.8 mm^3 (83.3–212.6) vs. 94.4 mm^3 (60.4–160.5) p = 0.06] lipid-rich and fibrous plaque volume [38.4 mm^3 (19.4–71.2) vs. 38.0 mm^3 (14.0–59.1), p = 0.11 and 50.4 mm^3 (26.1–77.6) vs. 42.1 mm^3 (31.1–60.3), p = 0.16] did not reach statistical significance. Lesions associated with ISR were more eccentric (n = 37, 86.0 % versus n = 159; p = 0.03) and more frequently demonstrated calcified portions on opposite sides on the vessel wall on cross-sectional datasets (i.e *headlight sign, see* Fig. 1; n = 24, 55.8 % versus n = 55, 23.4 %, p = 0.001). Out of 5 ISR-lesions that were further analyzed using OCT, stent malapposition was identified among the causes of ISR (see Fig. 3). FAI_{lesion} was significantly different in lesions with ISR as compared to those without ISR [−76.5 (−80.1 to −73.6) vs. −80.9 (−88.9 to −74.0), p = 0.02] (see Fig. 2 as well as Supplemental Table and Fig. 2). There was no difference concerning FAI_{RCA} between the two groups [−77.4 (−81.9 to −75.6) vs. −78.5 (−86.0 to −71.0), p = 0.41] (see Fig. 2). Using multivariate logistic regression analysis (OR and p-values for logistic regression are displayed in Table 2), lesion-specific FAI and the presence of the *headlight sign* turned out to predictors of ISR. An analysis of pericoronary FAI stratified into tertiles (low vs. mid vs. high) is shown in Supplemental Table 2. Mean value for high, moderate and low FAI was −70.5 ± 5.2, −80 ± 2.9 and −93.8 ± 6.5. Group differences were significant with a p-value of 0.042.

Table 1
Baseline patients' characteristics and medical treatment on admission.

	Patients w/o ISR (n = 175)	Patients with ISR (n = 34)	P-Value
Demographics			
Age, y	65.4 ± 10.6	65.1 ± 10.3	0.44
Male, n (%)	143 (81.7)	28 (82.4)	0.74
Weight, kg	84 ± 15.4	80.5 ± 13.5	0.15
Height, m	1.74 ± 0.09	1.74 ± 0.09	0.47
BMI, kg/m2	26.6 ± 3.7	27.7 ± 3.7	0.09
Risk factors			
Hypercholesterolemia, n (%)	68 (38.9)	17 (50.0)	0.95
Hypertension, n (%)	118 (67.4)	19 (55.9)	0.53
Smoking, n (%)	54 (30.9)	11 (32.4)	0.79
Family history of CAD, n (%)	49 (28.0)	3 (8.8)	0.15
Diabetes, n (%)	98 (56.0)	13 (38.2)	0.10
Laboratory findings			
Creatinine, mg/dl	0.89 ± 0.18	0.91 ± 0.16	0.36
C-reactive protein, mg/dl	2.99 ± 7.0	2.45 ± 2.37	0.34
Total cholesterol, mg/dl	200.94 ± 47.01	188.1 ± 45.64	0.15
Triglyceride, mg/dl	148.13 ± 102.73	148-00 ± 87.23	0.50
HDL cholesterol, mg/dl	56.6 ± 24.9	50.4 ± 15.86	0.05
LDL cholesterol, mg/dl	119.02 ± 41.66	110.57 ± 33.45	0.15
Hemoglobin A1c, (%)	5.86 ± 1.04	5.69 ± 0.46	0.16
Medication			
Aspirin, n (%)	56 (32.0)	12 (35.3)	0.68
Statin, n (%)	63 (36.0)	12 (35.3)	0.91
Beta-blocker, n (%)	60 (34.3)	7 (20.6)	0.34
ACEI and/or ARB, n (%)	68 (38.9)	9 (26.5)	0.49
Insulin, n (%)	2 (1.1)	1 (2.9)	0.88
OAD, n (%)	6 (3.4)	4 (11.8)	0.24

Data presented as mean ± standard deviation or absolute number (percentage). BMI = body-mass-index; CK = creatinine kinase; ACEI = angiotensin-converting enzyme inhibitor; ARB = angiotensin II receptor blocker; OAD = oral antidiabetic drugs.

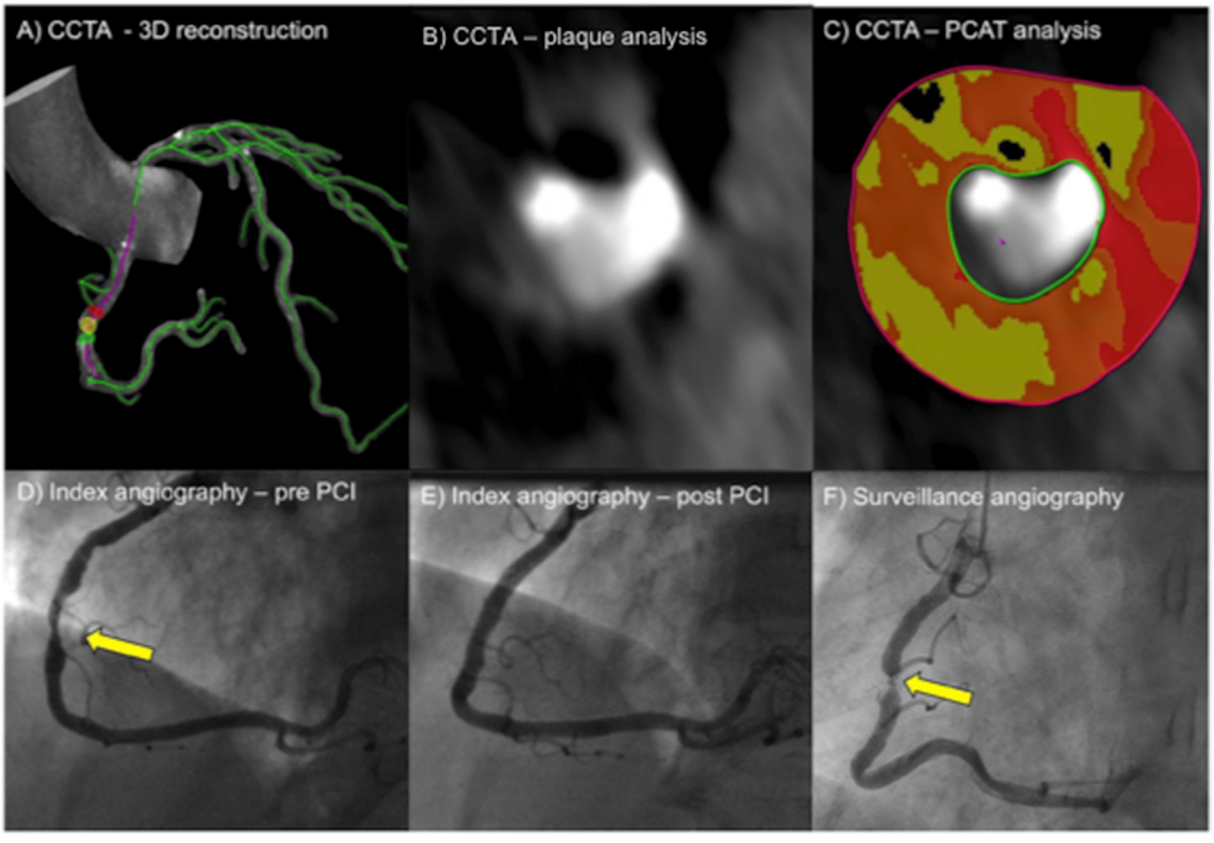

Fig. 1. Sample case of a 67 year old male patient with typical chest pain. CCTA showed a partially calcified lesion in the mid RCA and further plaque and pericoronary adipose tissue analysis was performed **(A–C)**. Subsequent invasive angiography (index angiography) revealed significant stenosis in the mid RCA **(D)**, which was successfully treated using percutaneous coronary intervention and stent placement (PCI) **(E)**. After 6 months, surveillance angiography demonstrated severe in-stent restenosis at the location where the *headlight-sign* was seen on CCTA **(F)**.

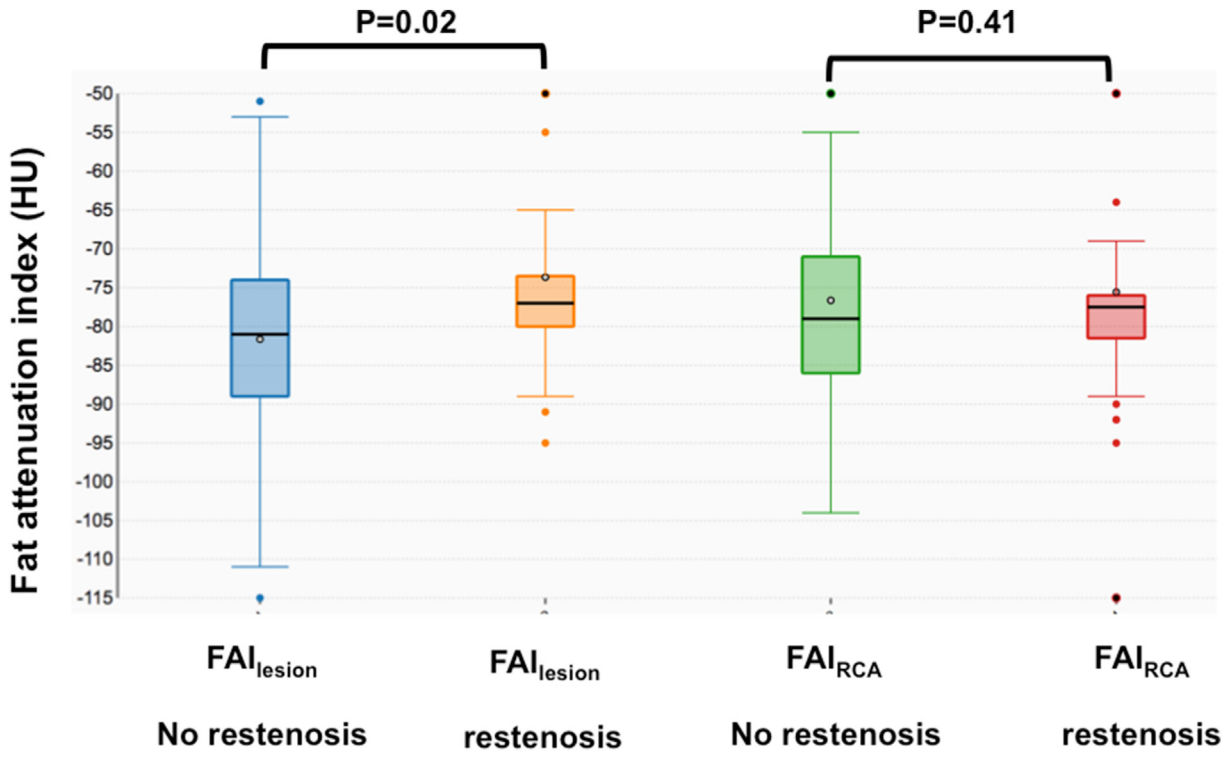

Fig. 2. Box and whisker plot of lesion specific and global PCAT assessment. Fat attenuation index of culprit lesions was significantly different in lesions with as compared to those without ISR [–76.5 (−80.1 to −73.6) vs. −80.9 (−88.9 to −74.0), $p = 0.02$]. There was no difference concerning fat attenuation index on the proximal RCA between the two groups [-77.4 (−81.9 to −75.6) vs. −78.5 (−86.0 to −71.0), $p = 0.41$].

4. Discussion

First, our findings demonstrate that the lesion - related perivascular fat attenuation index (FAI_{lesion}) but not the perivascular fat attenuation index around the proximal RCA, is increased in close proximity to coronary atherosclerotic lesions that are associated with in-stent restenosis on surveillance angiography, suggesting that coronary inflammation may be a potential driver of this kind of stent failure. Secondly, we found that exactly these lesions showed a certain arrangement of calcification at baseline such as being more eccentric. Thirdly, we introduce a novel nomenclature to a CT signature of calcified plaque eccentricity, that displayed two portions of calcification on opposite sides of the vessel wall on cross-sectional CT images: The *headlight sign* (i.e. we chose this name due to its resemblance of the bright front headlights of a car, see Supplemental Fig. 1) was seen more frequently in lesions that developed to in-stent restenosis. The overall findings of this study suggest that apart from coronary inflammation, morphologic factors such as the arrangement of calcification could be a contributing factor in the development of ISR. This is not in line with the findings of Tesche et al. who found that primarily lipid rich plaques were linked to ISR, suggesting that highly inflamed plaque at baseline even would cause a higher state of local inflammation after stent deployment that could lead to aggressive neointimal proliferation.[25]

The most common predictors of restenosis include small vessel size, increased stented length, complex lesion morphology, diabetes mellitus, and prior bypass surgery.[26] Apart from these patient-related and stent-related factors, predictors of ISR can be categorized into procedure - related factors, which include most notably stent underexpansion and malapposition.[6] So far, the only lesion-related markers that were identified to be independent predictors of restenosis based on pre-interventional angiographic and intravascular ultrasound (IVUS) measurements, were lesion length, plaque burden, plaque composition, and positive remodeling.[7,9] While this study cannot conclude how morphologic factors would affect ISR development, we hypothesize that a certain position of calcification could lead to unfavorable mechanical forces at the time of stent inflation, potentially affecting stent apposition as a result of the interaction of procedure-related (for instance inflation pressure etc.) and plaque-related factors such as dense calcification. This could either lead to obvious underexpansion of the stent at the very site of the eccentric calcified portion (as seen in Fig. 3) or to very discrete changes in stent strut penetration into lipid-rich areas in close proximity of the calcification causing an inflammatory reaction with consequently higher neointimal thickening, as already demonstrated by Farb et al..[7] This neointimal hyperplasia, caused by vessel wall injury due to the PCI, as well as neoatherosclerosis are regarded as the underlying basis for ISR.[24] However, other contributing factors to restenosis after vascular intervention involve several factors such as acute prolapse of the disrupted plaque, elastic recoil of the vessel wall and constrictive remodeling.[27]

Confirming the inflammatory hypothesis, the CANTOS trial (Canakinumab Anti-inflammatory Thrombosis Outcomes Study) revealed clinical data showing that targeting inflammation with an antibody against interleukin-1β after myocardial infarction was associated with lower incidence of recurrent cardiovascular events than placebo.[23] Consequently, targeted anti-inflammatory therapies may also be beneficial in patients with increased pre-procedural FAI_{lesion} values.

The occurrence of in-stent restenosis (ISR) remains a major limitation and may have an important impact on long-term prognosis after PCI.[28] Although the use of bare-metal-stents (BMS) was important in resisting acute and late constrictive mechanical forces as compared to balloon-angioplasty, the stent implantation procedure results in

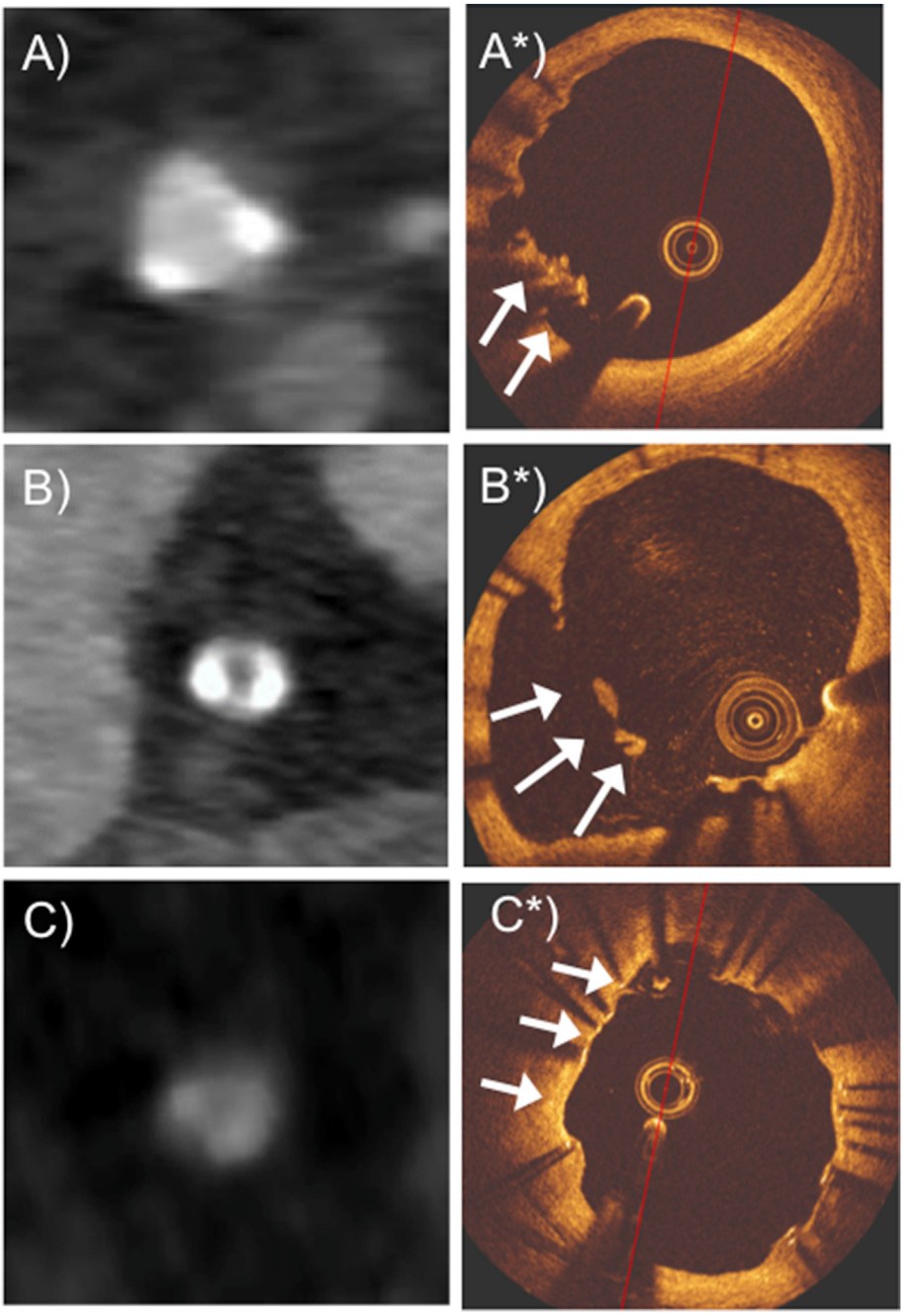

Fig. 3. Sample cases of 3 patients who underwent CCTA **(A–C)** and optical coherence tomography (OCT) **(A*-C*)** during surveillance angiography which revealed stent malapposition *(arrows)* contributing to in-stent-restenosis (ISR). In two of these cases, CCTA at baseline demonstrates eccentric calcification, including the headlight-sign, in close proximity to the site of maximum ISR at surveillance angiography.

increased acute vessel injury at the time of PCI and an enhanced inflammatory response to wound healing, leading to varying degrees of neointimal hyperplasia.[20] By inhibiting vascular smooth muscle migration, the introduction of drug-eluting stents (DES) led to a lower incidence of ISR as compared to BMS, with ISR rates of up to 5 % and 30 %, respectively.[21–23] While the presence of ISR, which is commonly defined as a re-narrowing of at least 50 % of the vessel diameter as determined by invasive catheterization,[24] can result in the recurrence of stable angina symptoms, it can also be a cause of acute coronary syndrome in up to a third of patients, which need treatment such as repeat catheter intervention (i.e. new generation DES or angioplasty with drug-coated balloons (DCB).[8,9] Hence, identification of patients at risk for ISR is an important undertaking.

Several limitations must be considered. This study was a retrospective with only a limited number of patients and not enough intravascular imaging data, so the exact mechanism of in-stent restenosis remains unclear. Additionally quantitative coronary angiography (QCA) measurements were not performed for restenosis assessment. However,

Table 2
Univariate and multivariate logistic regression of baseline CCTA characteristic for in-stent restenosis at surveillance angiography.

CCTA variable	No ISR Lesion $n = 235$	ISR Lesion $n = 43$	Univariate Analysis		Multivariate Analysis	
			OR (95%CI)	*P*-value	OR (95%CI)	*P*-value
Stenosis, %	74.0 ± 18.3	71.4 ± 20.6	0.991 (0.974–1.008)	0.300	1.004 (0.975–1.032)	0.808
MLA	1.70 (0.87–3.05)	1.91 (1.19–2.53)	1.023 (0.924–1.133)	0.659	1.074 (0.940–1.227)	0.295
Lesion length, mm	27.9 ± 9.8	27.6 ± 6.7	0.997 (0.962–1.032)	0.848	1.002 (0.928–1.082)	0.966
RI	1.05	0.99	0.728 (0.327–1.624)	0.438	0.467 (0.143–1.525)	0.207
Diffuse diseased, n (%)	90 (38.3)	22 (51.2)	1.676 (0.872–3.222)	0.121	1.590 (0.639–3.954)	0.318
Total PV (mm^2)	196.2 (126.4–314.9)	197.3 (150.4–332.4)	1.000 (0.998–1.002)	0.987	0.994 (0.988–1.001)	0.080
Calcified PV (mm^2)	94.4 (60.4–160.5)	129.8 (83.3–212.6)	1.001 (0.999–1.004)	0.205	1.008 (1.000–1.016)	0.053
Lipid-rich PV (mm^2)	38.4 (19.4–71.2)	38.0 (14.0–59.1)	0.997 (0.991–1003)	0.354	1.020 (0.982–1.059)	0.302
Fibrous PV (mm^2)	50.4 (26.1–77.6)	42.1 (31.1–60.3)	0.997 (0.989–1.004)	0.360	1.015 (0.996–1.035)	0.129
Spotty calcification n (%)	108 (46.0)	21 (48.8)	1.122 (0.586–2.152)	0.728	1.685 (0.667–4.254)	0.270
Eccentric calcification n (%)	159 (67.7)	37 (86.0)	2.948 (1.193–7.285)	**0.019**	3.634 (0.848–15.487)	0.082
Homogenous n (%)	92 (39.1)	22 (51.2)	1.628 (0.848–3.128)	0.143	1.931 (0.769–4.848)	0.161
Headlight n (%)	55 (23.4)	24 (55.8)	4.134 (2.108–8.106)	**<0.001**	4.284 (1.753–10.472)	**0.001**
FAI_{lesion}	−80.9 (−88.9 to −74.0)	−76.5 (−80.1 to −73.6)	1.045 (1.010–1.081)	**0.011**	1.089 (1.032–1.148)	**0.002**
FAI_{RCA}	−78.5 (−86.0 to −71.0)	−77.4 (−81.9 to −75.6)	1.002 (0.987–1.016)	0.799	0.955 (0.910–1.003)	0.064

MLA, minimal lumen area; RI, remodeling index; PV, plaque volume; FAI, fat attenuation index.

coronary lesions were graded qualitatively by the clinicians and according to the clinical symptoms of the patients. On this basis, the interventional cardiologist made the decision to perform PCI.

5. Conclusions

Coronary lesions associated with ISR at surveillance angiography demonstrated differences in the arrangement of calcified portions as well as an increased lesion-specific pericoronary fat attenuation index at baseline CCTA. This latter finding suggests that preprocedural perivascular inflammation at baseline may play a major role in the development of in-stent restenosis.

Disclosures

No funding was received for conducting this study.

Declaration of competing interest

On behalf of the co-authors, I declare that there are no conflicts of interests associated with our manuscript.

Appendix A. Supplementary data

Supplementary data to this article can be found online at https://doi.org/10.1016/j.jcct.2024.09.010.

References

1. Lawton JS, Tamis-Holland JE, Bangalore S, et al. 2021 ACC/AHA/SCAI guideline for coronary artery revascularization: a report of the American College of Cardiology/American Heart Association Joint Committee on Clinical Practice Guidelines. *Circulation*. 2022;145:18e114.
2. Madhavan MV, Kirtane AJ, Redfors B, et al. Stent-related adverse events >1 Year after percutaneous coronary intervention. *J Am Coll Cardiol*. 2020;75:590–604.
3. Bønaa KH, Mannsverk J, Wiseth R, et al. Drug-eluting or bare-metal stents or coronary artery disease. *N Engl J Med*. 2016;375:1242–1252.
4. James SK, Stenestrand U, Lindbäck J, et al. Long-term safety and efficacy of drug-eluting versus baremetal stents in Sweden. *N Engl J Med*. 2009;360:1933–1945.
5. Cassese S, Byrne RA, Tada T, King LA, Kastrati A. Clinical impact of extended dual antiplatelet therapy after percutaneous coronary interventions in the drug-eluting stent era: a meta-analysis of randomized trials. *Eur Heart J*. 2012;33(24):3078–3087.
6. Byrne RA, Joner M, Kastrati A. Stent thrombosis and restenosis: what have we learned and where are we going? The Andreas Grüntzig Lecture ESC 2014. *Eur Heart J*. 2015;36(47):3320–3331.
7. Farb A, Weber DK, Kolodgie FD, Burke AP, Virmani R. Morphological predictors of restenosis after coronary stenting in humans. *Circulation*. 2002;105:2974e2980.
8. Hoffmann R, Mintz GS, Mehran R, et al. Intravascular ultrasound predictors of angiographic restenosis in lesions treated with Palmaz-Schatz stents. *J Am Coll Cardiol*. 1998;31:43e49.
9. Sahara M, Kirigaya H, Oikawa Y, et al. Arterial remodeling patterns before intervention predict diffuse in-stent restenosis: an intravascular ultrasound study. *J Am Coll Cardiol*. 2003;42:1731e1738.
10. Kornowski R, Hong MK, Tio FO, Bramwell O, Wu H, Leon MB. In-stent restenosis: contributions of inflammatory responses and arterial injury to neointimal hyperplasia. *J Am Coll Cardiol*. 1998;31:224–230.
11. Welt FG, Rogers C. Inflammation and restenosis in the stent era. *Arterioscler Thromb Vasc Biol*. 2002;22:1769–1776.
12. Antoniades C, Antonopoulos AS, Deanfield J. Imaging residual inflammatory cardiovascular risk. *Eur Heart J*. 2020;41:748–758.
13. Wolf D, Ley K. Immunity and inflammation in atherosclerosis. *Circ Res*. 2019;124:315–327.
14. Lin A, Dey D, Wong DTL, Nerlekar N. Perivascular adipose tissue and coronary atherosclerosis: from biology to imaging phenotyping. *Curr Atheroscler Rep*. 2019;21:47.
15. Ohyama K, Matsumoto Y, Amamizu H, et al. Association of coronary perivascular adipose tissue inflammation and drug-eluting stent-induced coronary hyperconstricting responses in pigs: F-fluorodeoxyglucose positron emission tomography imaging study. *Arterioscler Thromb Vasc Biol*. 2017;37:1757–1764.
16. Wang J, Chen D, Cheng XM, et al. Influence of phenotype conversion of epicardial adipocytes on the coronary atherosclerosis and its potential molecular mechanism. *Am J Transl Res*. 2015;7:1712–1723.
17. Crewe C, An YA, Scherer PE. The ominous triad of adipose tissue dysfunction: inflammation, fibrosis, and impaired angiogenesis. *J Clin Invest*. 2017;127:74–82.
18. Oikonomou EK, Antonopoulos AS, Schottlander D, et al. Standardized measurement of coronary inflammation using cardiovascular computed tomography: integration in clinical care as a prognostic medical device. *Cardiovasc Res*. 2021;117(13):2677–2690.
19. Oikonomou EK, Marwan M, Desai MY, et al. Non-invasive detection of coronary inflammation using computed tomography and prediction of residual cardiovascular risk (the CRISP CT study): a post-hoc analysis of prospective outcome data. *Lancet*. 2018;392:929–939.
20. Leipsic J, Abbara S, Achenbach S, et al. SCCT guidelines for the interpretation and reporting of coronary CT angiography: a report of the Society of Cardiovascular Computed Tomography Guidelines Committee. *J Cardiovasc Comput Tomogr*. 2014;8:342e358.
21. Jacobs JE, Boxt LM, Desjardins B, et al. ACR practice guideline for the performance and interpretation of cardiac computed tomography (CT). *J Am Coll Radiol*. 2006;3:677e685.
22. Austen WG, Edwards JE, Frye RL, et al. A reporting system on patients evaluated for coronary artery disease. Report of the Ad Hoc Committee for Grading of Coronary Artery Disease, Council on Cardiovascular Surgery, American Heart Association. *Circulation*. 1975;51(4 Suppl):5–40.

23. Voros S, Rinehart S, Qian Z, et al. Coronary atherosclerosis imaging by coronary CT angiography: current status, correlation with intravascular interrogation and meta-analysis. *JACC Cardiovasc Imaging*. 2011;4:537e548.
24. Achenbach S, Ropers D, Hoffmann U, et al. Assessment of coronary remodeling in stenotic and nonstenotic coronary atherosclerotic lesions by multidetector spiral computed tomography. *J Am Coll Cardiol*. 2004;43:842e847.
25. Tesche C, De Cecco CN, Caruso D, et al. Coronary CT angiography derived morphological and functional quantitative plaque markers correlated with invasive fractional flow reserve for detecting hemodynamically significant stenosis. *J Cardiovasc Comput Tomogr*. 2016;10(3):199–206.
26. Cassese S, Byrne RA, Schulz S, et al. Prognostic role of restenosis in 10 004 patients undergoing routine control angiography after coronary stenting. *Eur Heart J*. 2015; 36(2):94–99.
27. Byrne RA, Joner M, Alfonso F, Kastrati A. *Treatment of In-Stent Restenosis. Interventional Cardiology: A Companion to Braunwald's Heart Disease*. Elsevier; 2015.
28. Antonopoulos AS, Sanna F, Sabharwal N, et al. Detecting human coronary inflammation by imaging perivascular fat. *Sci Transl Med*. 2017;9:eaal2658.